

General Relativistic Self-Similar Solutions in Cosmology

Adi Nusser

Physics Department- Technion, Haifa 32000, Israel

7 March 2018

ABSTRACT

We present general relativistic solutions for self-similar spherical perturbations in an expanding cosmological background of cold pressure-less gas. We focus on solutions having shock discontinuities propagating in the surrounding cold gas. The pressure, p , and energy-density, μ , in the shock-heated matter are assumed to obey $p = w\mu$, where w is a positive constant. Consistent solutions are found for shocks propagating from the symmetry center of a region of a positive density excess over the background. In these solutions, shocks exist outside the radius marking the event horizon of the black hole which would be present in a shock-less collapse. For large jumps in the energy-density at the shock, a black hole is avoided altogether and the solutions are regular at the center. The shock-heated gas does not contain any sonic points, provided the motion of the cold gas ahead of the shock deviates significantly from the Hubble flow. For shocks propagating in the uniform background, sonic points always appear for small jumps in the energy-density. We also discuss self-similar solutions without shocks in fluids with $w < -1/3$.

Key words: cosmology: theory, large-scale structure of the Universe — relativity

1 INTRODUCTION

Detailed studies of generic self-gravitating systems are only possible with the aid of complex numerical methods. Part of the complication arises from the long range nature of gravitational interactions. Thus, even equilibrium states, when they exist, do not in general obey standard statistical mechanics. This is correct for both Newtonian gravity as well as general relativity (GR), but the latter adds its peculiar technical and conceptual challenges. Analytic or semi-analytic treatment of systems possessing special symmetries are, therefore, of great interest. Gravity is the dominant force dictating the growth of structure in the universe. Thus, self-gravitating perturbations in an expanding cosmological has traditionally gained a great deal of attention (cf. Peebles 1990). Here we present a class of solutions which describe the evolution of spherical perturbations in an expanding Einstein-de Sitter cosmological background. We focus on the evolution of self-similar perturbations in GR. Self-similarity occurs when dimensionless physical variables can be expressed as functions of some combination of the time and space coordinates. Self-similar systems offer great simplification since they are described by ordinary differential equations. Newtonian treatment of cosmological self-similar perturbations have been presented in great detail

previously in the literature (e.g. Fillmore & Goldreich 1984; Bertschinger 1985; Chuzhoy & Nusser 2000). Nevertheless, it is instructive to review the general features of these solutions. In cosmology, we assume that the density fluctuations are extremely small at time, t_i , close to the the Big Bang singularity. An isolated small density perturbation having the form $\delta\mu \sim r^{-s}$ (r is the distance from the symmetry center) at t_i , develops a self-similar behavior at sufficiently late times, $t \gg t_i^*$. Consider first a positive density perturbation in a universe made solely of dust (i.e. collision-less matter). As time goes-by a shell of matter begins to expand at a rate lower than the background until it reaches a maximum distance from the center. The shell then falls inward and ends up oscillating around the center together with shells which have reached it at earlier times. According to this picture, the radius, r_1 , of the shell which is at maximum expansion at time t plays an important role. For $r > r_1$, matter is still expanding, while at $r \ll r_1$ shells of matter are oscillating in the central potential well generated by their self-gravity. The self-similar variable can then be taken to be the ratio,

* An additional assumption which is often made is that the initial expansion rate of matter at r is equal to that of the unperturbed background. This assumption is, however, unnecessary as long as the deviations from the background expansion rate are not great.

$r/r_1(t)$. For a universe filled with a collisional fluid (gas), self-similarity develops provided the initial pressure is negligible and that the gas is able to shock and evolve adiabatically. In this case, an inner region of hot shocked gas develops. The shock bounding this region propagates away from the center at a rate $dr_1(t)/dt$.

Self-similarity in GR is obtained for a more restricted class of initial perturbations than in Newtonian gravity. GR admits self-similar solutions only for specific values of the power law index s , while Newtonian dynamics does not impose such restrictions. Further, the pressure, p , must be related linearly to the energy-density, μ , of matter (Cahil & Taub 1971). Carr & Hawking (1974) and Carr & Yahil (hereafter CY90) have studied self-similar perturbations in an expanding universe. Their treatment, however, did not include shocks which might form as a result of collapse or energy injection into the system. Here we complement the work of CY90 by exploring solutions which involve shock discontinuities. We assume that the isotropic cosmic background is made of cold pressure-less matter that is able to shock. We will present solutions in which shocks propagate from a central point into the uniform cosmic background or into the outer regions of a perturbation with positive excess of energy-density in the cold gas. Shock-heated gas will be assumed to obey the equation of state $p = w\mu$ ($w > 0$). We also present solutions with no shocks for $w < -1/3$, a case which has not been discussed at length in the literature before.

The paper is organized as follows. In §2 we summarize GR equations for self-similar perturbations in comoving coordinates. For a detailed discussion of these equations we refer the reader to CY90 and Carr & Coley (2000) (hereafter CC02). In §3 we discuss the formation of shocks and the jump conditions relating the physical variables on both sides of the shock discontinuity. In §4 we present full numerical solutions. We conclude with a general discussion in §5.

2 THE SELF-SIMILAR GR EQUATIONS IN SPHERICAL SYMMETRY

We work with comoving coordinates as they are particularly convenient for the study of cosmological perturbations. With only minor changes of notation our description of the equations closely follows CY90 and CC02. Denoting the time, the radius and the two spherical angular coordinates by t , r , θ and ϕ , the space-time metric is expressed in terms of the interval ds^2 as (e.g. Landau & Lifshitz 1975),

$$ds^2 = e^{2\nu} dt^2 - e^{2\lambda} dr^2 - R^2 d\Omega^2, \quad (1)$$

where ν , λ and R are, in general, functions of t and r , and $d\Omega^2 = d\theta^2 + \sin^2\theta d\phi^2$. In comoving coordinates the energy-momentum tensor has the form $T^{\mu\nu} = (\mu + p)u^\mu u^\nu - pg^{\mu\nu}$ where $u^\mu = dt/ds = (e^{-\nu}, 0, 0, 0)$. For an equation of state $p = w\mu$ where w is a constant, self-similar solutions in which

dimensionless variables are functions of $z \equiv r/t$ alone can be obtained. We use the following dimensionless variables[†],

$$S(z) \equiv \frac{R}{r}, \quad \xi(z) \equiv (\mu r^2)^{-1/(1+w)} \quad \text{and} \quad M(z) \equiv \frac{m}{R}, \quad (2)$$

where

$$m(r, t) = \frac{R}{2} \left[1 + e^{-2\nu} \left(\frac{\partial R}{\partial t} \right)^2 - e^{-2\lambda} \left(\frac{\partial R}{\partial r} \right)^2 \right]. \quad (3)$$

Using $T_{\beta;\alpha}^\alpha = 0$, gives $\partial_t \lambda + 2\partial_t R/R = -2\partial_t \mu/(p + \mu)$ and $\partial_r \nu = -2\partial_r p/(p + \mu)$. For $p = w\mu$, these equations yield

$$e^\nu = \beta \xi^w z^{2w/(1+w)} \quad \text{and} \quad e^{-\lambda} = \gamma \xi^{-1} S^2, \quad (4)$$

Substituting these relations in the remaining Einstein equations and using $\partial/\partial t = -(z/t)d/dz$ and $\partial/\partial r = (z/r)d/dz$ yield

$$\ddot{S} + \dot{S} + [S + (1+w)\dot{S}] \left(\frac{2}{1+w} \frac{\dot{S}}{S} - \frac{\dot{\xi}}{\xi} \right) = 0, \quad (5)$$

$$\begin{aligned} \left(\frac{2w\gamma^2}{1+w} \right) S^4 + \frac{2}{\beta^2} \frac{\dot{S}}{S} \xi^{2-2w} z^{(2-2w)/(1+w)} \\ - (V^2 - w) \gamma S^4 \frac{\dot{\xi}}{\xi} = (1+w) \xi^{1-w}, \end{aligned} \quad (6)$$

$$M = S^2 \xi^{-(1+w)} \left[1 + (1+w) \frac{\dot{S}}{S} \right], \quad (7)$$

$$M = \frac{1}{2} + \frac{1}{2\beta^2} \xi^{-2w} z^{2(1-w)/(1+w)} - \frac{1}{2} \gamma^2 \xi^{-2} S^6 \left(1 + \frac{\dot{S}}{S} \right), \quad (8)$$

and

$$V = (\beta\gamma)^{-1} \xi^{1-w} S^{-2} z^{(1-w)/(1+w)}, \quad (9)$$

where an over-dot denotes a derivative with respect to $y = \ln z$.

A particular solution of these equations describes the Einstein-de Sitter universe, i.e. the flat critical density Friedmann-Robertson-Walker (FRW) uniform density background. This solution is

$$\xi = z^{-2/(1+w)}, \quad S = z^{-2/(3+3w)}, \quad (10)$$

with

$$\beta = \frac{\sqrt{2}}{\sqrt{3}(1+w)}, \quad \gamma = \frac{3+3w}{1+3w}. \quad (11)$$

The space-time interval is

$$ds^2 = \beta^2 dt^2 - \gamma^{-2} z^{-4/(3+3w)} dr^2 - r^{2(1+3w)/(3+3w)} t^{4/(3+3w)} d\Omega^2. \quad (12)$$

This is brought to a standard form

$$ds^2 = d\tilde{t}^2 - \tilde{r}^{4/(3+3w)} (d\tilde{r}^2 + \tilde{r}^2 d\Omega^2) \quad (13)$$

using the transformation

$$\tilde{t} \equiv \beta t \quad \text{and} \quad \tilde{r} = \beta^{-2/(3+3w)} r^{(1+3w)/(3+3w)}. \quad (14)$$

[†] The variable ξ defined here is related to $x(z)$ in CY90 by $\xi^{1/w}$.

2.1 Equations in perturbed variable

In order to describe deviations from the isotropic FRW background, we follow CY90 and introduce $A(z)$ and $B(z)$ according to[‡]

$$\xi \equiv z^{-2/(1+w)} e^A, \quad S \equiv z^{-2/(3+3w)} e^B. \quad (15)$$

From the definition of ξ in (2), we get $\mu t^2 = e^A$. Thus, to linear order A can be identified as the energy-density contrast $\delta\mu/\mu$. The equations (5) through (8), expressed in terms of A and B , are,

$$\ddot{B} = \frac{1}{3}\dot{A} + (1+w)\dot{A}\dot{B} - 3\dot{B}^2 - \left(\frac{1+3w}{1+w}\right)\dot{B}, \quad (16)$$

$$\dot{B} = \frac{1}{2}\dot{A} \left(1 - \frac{w}{V^2}\right) + \frac{1}{3+3w} [e^{(w-1)A} - 1], \quad (17)$$

$$M = \left[\frac{1}{3} + (1+w)\dot{B}\right] e^{2B-(1+w)A} z^{2(1+3w)/(3+3w)}, \quad (18)$$

$$M = \frac{1}{2} + \frac{3(1+w)^2}{4} e^{2B-2wA} z^{2(1+3w)/(3+3w)} \left[\dot{B} - \frac{2}{3(1+w)}\right]^2 \quad (19)$$

$$-\frac{9(1+w)^2}{2(1+3w)^2} \left[\dot{B} + \frac{1+3w}{3(1+w)}\right]^2 e^{6B-2A}, \quad (20)$$

and

$$V = \left(\frac{1+3w}{\sqrt{6}}\right) z^{(1+3w)/(3+3w)} e^{(1-w)A-2B}. \quad (21)$$

2.2 Asymptotic solutions

Linear perturbations describing small deviations from uniformity are obtained for $A \sim \delta\mu/\mu \ll 1$ and $\dot{B} \ll 1$. The linearized equations have two solutions. The first is (CY90)

$$A_1 = -\frac{1+3w}{1+w} k z^{-2(1+3w)/(3+3w)}, \quad (22)$$

$$B_1 = B_\infty - k z^{-2(1+3w)/(3+3w)}, \quad (23)$$

where the constants B_∞ and k are related by

$$k = \frac{3(1+w)(e^{-2B_\infty} - e^{4B_\infty})}{2(1+3w)(5+3w)}. \quad (24)$$

Expressed in terms of the FRW coordinates \tilde{r} and \tilde{t} given in (14), we see that $A_1 \sim \delta\mu/\mu \propto \tilde{r}^{-2} \tilde{t}^{2(1+3w)/(3+3w)}$. Therefore, the energy-density contrast, $\delta\mu/\mu$, is \tilde{r}^{-2} , independent of w , and has a temporal behavior identical to that obtained for large scale perturbations in the standard linear perturbation theory in the comoving gauge (e.g. Peebles 1993). The second solution is

$$A_2(z) \propto z^{(1-w)/(1+w)} \quad \text{and} \quad B_2(z) = \frac{A_2(z)}{6}. \quad (25)$$

According to (14), the limit $\tilde{r} \rightarrow \infty$ corresponds to $z \rightarrow \infty$ and $z \rightarrow 0$, respectively for $w > -1/3$ and $-1 < w < -1/3$. Therefore, density perturbations approaching zero as $\tilde{r} \rightarrow \infty$ are described by A_1 for $w > -1/3$ and A_2 for $-1 < w < -1/3$. The mode A_1 grows with time, while A_2 decays.

[‡] Note that the A is equal to w times the function used by CY90.

3 SHOCKS

We will consider solutions involving shock discontinuities propagating in a medium of cold pressure-less gas. We will assume that the heated matter behind the shock obeys the equation of state $p = w\mu$. A shock will be specified by the ratio of the energy-densities on both of its sides. The remaining hydrodynamical variables and the components of the metric on both sides of the shock are then related by means of the jump conditions. These are usually derived by working first with Schwarzschild coordinates where the metric tensor is continuous and then transforming back to comoving coordinates (Bardeen 1965; Cahil & Taub 1971). Quantities just ahead and behind the shock are denoted by the (+) and (-) symbols, respectively. The general form of the jump conditions in comoving coordinates is (Cahil & Taub 1971),

$$R_+ = R_- \quad (26)$$

$$V_+^2 = \frac{(w-\mu_- - w+\mu_+)(\mu_- + w+\mu_+)}{(\mu_- - \mu_+)(\mu_+ + w-\mu_-)} \quad (27)$$

$$V_-^2 = \frac{(w-\mu_- - w+\mu_+)(\mu_+ + w-\mu_-)}{(\mu_- - \mu_+)(\mu_- + w+\mu_+)} \quad (28)$$

$$e^{2\nu_- - 2\nu_+} = \frac{(\mu_- + w+\mu_+)(\mu_+ + w+\mu_+)}{(\mu_+ + w-\mu_-)(\mu_- + w-\mu_-)} \quad (29)$$

$$e^{2\lambda_- - 2\lambda_+} = \frac{(\mu_+ + w-\mu_-)(\mu_+ + w+\mu_+)}{(\mu_- + w+\mu_+)(\mu_- + w-\mu_-)} \quad (30)$$

$$\Gamma_- = \frac{C + \Gamma_+}{1 + C\Gamma_+} \quad (31)$$

where

$$\Gamma = e^{\lambda-\nu} \frac{\partial R/\partial t}{\partial R/\partial r} \quad \text{and} \quad C = \frac{V_+ - V_-}{1 - V_- V_+} \quad (32)$$

The condition (26) leads to the continuity of the self-similar variable S , i.e. $S_+ = S_-$. Using the relations

$$R_t = r S_t = r \frac{dS}{dz} \frac{dz}{dt} = -z \dot{S},$$

$$R_r = S + r S_r = S + r \frac{dS}{dz} \frac{dz}{dr} = S + \dot{S}.$$

we find that

$$\Gamma = \frac{-V(s)\dot{S}}{S + \dot{S}}. \quad (33)$$

Therefore, the condition (31) relates between $\dot{S} = z dS/dz$ on both sides of the shock.

4 NUMERICAL SOLUTIONS

We present here numerical solutions of the equations of motion for cases with and without shocks. The boundary conditions for all solutions obey the asymptotic form giving small density perturbations in the limit of large FRW coordinate \tilde{r} , corresponding to $z \gg 1$ $w > -1/3$ and to $z \ll 1$ for $w < -1/3$.

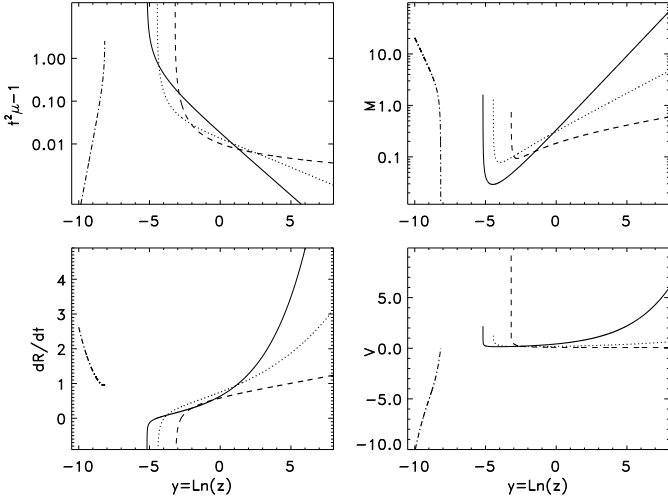


Figure 1. Numerical solutions of self-similar positive density perturbations in a FRW universe for $w = 0$ (solid lines), -0.2 (dotted), -0.3 (dashed) and -0.6 (dash-dotted). *Top-left:* the excess energy-density in units of the background value. *Top-right:* the function $M = S/R$. *Bottom-left:* the fluid “velocity” $dR/dt = -z^2 dS/dz$. *Bottom-right:* the velocity V of surfaces of constant z relative to the fluid. For $w = -0.6$, the lines showing M , dR/dt and V are scaled down by factors of 10^4 , 500 and 25 , respectively.

4.1 Solutions without shocks

The case $w > 0$ has been considered extensively by CY90. Therefore, we only present solutions for $-1 < w < 0$. An important difference between solutions with $w > 0$ and $w < 0$ is the following. For $w > 0$, a sonic point at which $V = w^{-1/2}$ may exist. At this point the term $(1 - w/V^2)$ in equation (17) vanishes, leaving \dot{A} undetermined. Certain physical assumptions must then be made in order to complete the solution across the sonic point (e.g. Ori & Piran 1990; CY90). For $w < 0$, sonic points do not exist and, barring singularities, \dot{A} is always determined by (17).

Figure 1 shows results of numerical integration of a positive density perturbation for $w = 0$ (solid lines), $w = -0.2$ (dotted), $w = -0.3$ (dashed), and $w = -0.6$ (dash-dotted). The four panels show, from top-left in clockwise order, the contrast in the energy-density (i.e. $\mu/\bar{\mu} - 1$ where $\bar{\mu}$ is the background energy density), the function $M = m/R$, the “velocity” $dR/dt = -z^2 dS/dz$, and the velocity V of surfaces of constant z relative to the fluid. Solutions with $w > -1/3$ diverge at a finite value of z . This singular behavior of the solutions indicates the presence of black holes with apparent horizon at the point with $M = 1/2$ and an event horizon at the point with $V = 1$ (Carr & Hawking 1974). Comoving coordinates should allow a description of the physical variables down to the singularity at the center. For the solutions with $w > -1/3$, the finite value of z at which the solutions diverge represents the shell having a comoving coordinate r and arriving at the center at time $t = r/z$ (e.g. Landau & Lifshitz 1975). The lines of $t^2\mu - 1$ follow the asymptotic form $z^{(1-w)/(1+w)}$ at $z \ll 1$

for $w < -1/3$ and $z^{2(1+3w)/(3+3w)}$ at $z \gg 1$ for $w > -1/3$. For $w < -1/3$, the limit $z \rightarrow 0$ is obtained by taking the limit $\tilde{r} \rightarrow \infty$ or/and $t \rightarrow \infty$. Therefore, the self-similar solution for $w = -0.6$ describes a mode which decays with time and approaches zero at large FRW coordinate \tilde{r} , in contrast to the solutions shown for $w > -1/3$ which grow with time. In the Newtonian limit the quantity dR/dt describes the velocity of a shell relative to a central observer. For $w > -1/3$, at sufficiently large z , dR/dt is positive. As we decrease z , dR/dt changes signs, indicating the collapse of matter towards the center.

4.2 Solutions with shocks

We discuss now solutions describing self-similar perturbations in the presence of shocks. The cosmic background is assumed to be made of cold pressure-less gas which is able to shock. We focus first on shocks propagating from the center of a perturbation with positive energy-density excess in the cold gas. At the end of this section we present solutions for shocks propagating into the uniform density background. The equations of motion (16) and (17) with $w = 0$ are integrated inward from $z_1 \gg 1$ with initial conditions dictated by the linear solution. The integration gives tabulated values for the variables $A(z)$ and $B(z)$ from z_1 until $z = z_s$ ($z_s < z_1$), where a shock is assumed to exist. Given the variables A_+ and B_+ just a head of the shock at z_s we obtain the corresponding physical variables ν_+ , λ_+ , S_+ and ξ_+ . Then, assuming a value for the ratio $g = \mu_-/\mu_+$ of the energy-densities behind and ahead of the shock, we use the jump conditions (26) through (31) to obtain ν_- , λ_- , S_- and ξ_- behind the shock. These variables are then used as initial conditions in the numerical integration of the equations (5) and (6), from z_s down to smaller values. This is done for several values g and z_s . The condition (27) implies that shocks cannot exist at points with $V > 1$. This is related to that fact that $V = 1$ marks an event horizon inner to which matter must eventually hit the central singularity (Carr & Hawking 1974). Results of the numerical integrations are shown in figure (2). The top-left panel plots the energy-density (in units of the background value), $t^2\mu$. The dashed line represents the solution obtained for the shock-less collapse of cold gas ($w = 0$). The solid lines show $t^2\mu$ versus z when shocks are assumed to exist at $\ln z_s = -3.46$ and $\ln z_s = -4.05$. For these z_s , the shock-less solution has $dR/dt < 0$ (the bottom panel to the left). For each value of z_s , lines representing solutions obtained for four values of $g = \mu_-/\mu_+$ are shown: $g = 1.1, 2, 3,$ and 5 . At both z_s , the energy-density reaches a constant value as $z \rightarrow 0$ for the two larger values of g and diverges at a finite z for the smaller values. Given g , the jump conditions determine the pressure and energy-density ahead of the shock and, therefore, the ratio $w = w_- = p_-/\mu_-$. The top-right panel plots lines of w versus g for three values of $y_s = \ln z_s$ as indicates in the figure. The behavior of these lines can be easily understood by a straightforward algebraic manipulation of the jump condition (27) with $w_+ = 0$. For g close to unity, w increases linearly with $g - 1$. In the limit $g \gg 1$ we get $w \approx V_+^2/(1 - V_+^2)/g$ so that $p_- = w\mu_-$ which is indepen-

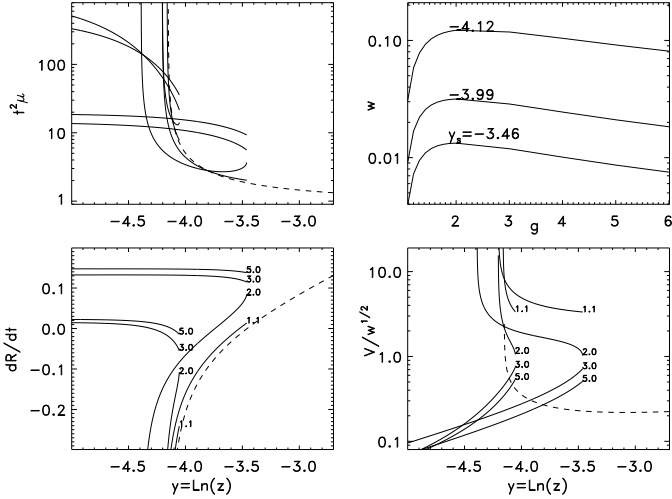


Figure 2. Results of numerical integration of the equations in the presence of shocks propagating from the center of a positive density excess. The dashed lines in the top-left, bottom-left and bottom-right panels correspond to the shock-less collapse of cold gas ($w = 0$). The solid lines in these panels represent the physical variables in the shock-heated region. Results are shown for shocks present at $z_s = -3.46$ and $z_s = -4.05$; for $g = \mu_-/\mu_+ = 1.2, 2, 3,$ and 5 at each z_s . For these values of z_s the shock-less solution has $dR/dt < 0$. *Top-left:* the energy-density in units of the background density versus the variable $y = \ln z$. *Top-right:* the parameter w in the shocked material as a function of the assumed g , for shocks at three values of z_s as indicated in the figure. *Bottom-left:* the “velocity” $dR/dt = -z^2 dS/dz$. *Bottom-right:* the velocity V of constant z surfaces relative to the fluid, where the dashed line is the actual velocity of the collapsing cold gas ($w = 0$), while the solid lines show $V/w^{1/2}$.

dent of g . Curves of dR/dt are shown in the bottom-left panel. The numeric labels on each line indicate the corresponding value of g . It is interesting that for the regular solutions, dR/dt converges to a positive constant as $z \rightarrow 0$. This constant becomes smaller with decreasing z_s and we conjecture that it will approach zero as z_s gets very close to the event horizon marked by the point with $V = 1$ in the dashed curve (bottom panel to the left). The physical interpretation of this is that outflows/winds from a central region are required for the formation of shocks. The intensity of these outflows determine the location of the shock, z_s . The bottom-right panel plots the velocity V versus z . The actual velocity is shown for the cold collapse (dashed) while the ratio $V/w^{1/2}$ is plotted for the other lines. For the regular solutions, $V/w^{1/2}$ is less than unity throughout the shocked regions. The other solutions have $V/w^{1/2} > 1$ over the range from z_s down to the finite z marking the central singularity. Thus, in both cases no sonic points exist. Finally, the asymptotic behavior of the numerical solutions near the center is consistent with the analysis of CC02. For the regular solutions, we have $V \rightarrow 0$ as $z \rightarrow 0$. The analysis of CC02 of this case gives $S \propto z^{-1}$ and $\xi \propto z^{-2/(1+w)}$ which according to (2) implies $t^2\mu = const$ and $dR/dt = -z^2 dS/dz = const$. Our solutions match this behavior extremely well.

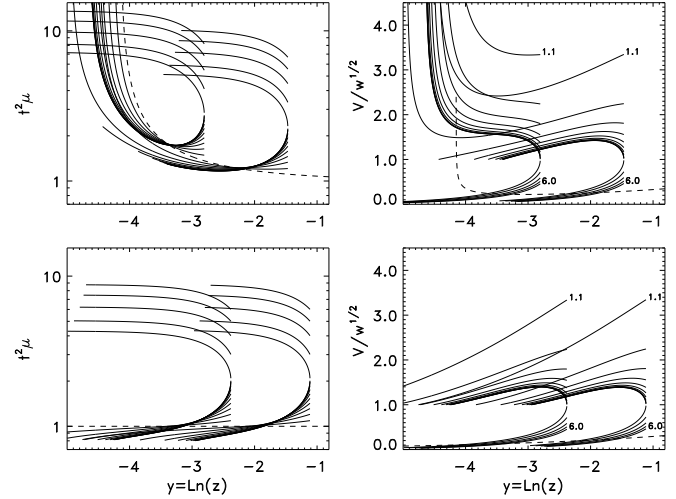


Figure 3. Comparison between solutions for shocks propagating in the uniform cosmic background (bottom panels) and in a positive density excess over the background (top). In all panels, dashed lines represent solutions without shocks, while the solid ones correspond to shocks assumed to exist at two different positions. The solid lines at each shock position correspond to several values of $g = \mu_-/\mu_+$ from $g = 1.1$, to 6 in equal steps of 0.1 . Left panels show lines of energy-density versus $y = \ln z$. Right panels: show $V/w^{1/2}$ for the solid lines and the actual the velocity V for the dashed line.

It is interesting to compare between the solutions for shocks propagating in a positive density perturbation and in the uniform background. These solutions are represented, respectively, in the top and bottom rows of in figure (??). The positive density solutions are taken from the output of the integration used in figure (2) but for shocks assumed to exist at two points outside the region with $dR/dt < 0$ (compare with figure (2)). This means that the shock exist at a point where the cold fluid is expanding. Physically this is possible if a central energy source is present. As is seen in the top panel to the right, solid curves with intermediate g hit sonic points ($V = w^{1/2}$). At these points we stop the integration. Larger values of g yield regular solutions without sonic points. For smaller g , the velocity V changes direction and tends to infinity, indicating the presence of a black hole. As z_s is decreased, the solutions behave in a manner similar to what we have seen in figure (2). In the uniform background case, sonic points always exist for small g and disappear for sufficiently large values.

5 DISCUSSION

In the standard cosmological model, the universe on large scales is nearly uniform so that super-horizon perturbations are well described by the general relativistic theory of linear perturbations (e.g. Bardeen 1980). However, in view of recent observational data, it seems that GR might be needed for a full study of perturbations on small scales where strictly speaking the linearized equations are invalid. These data

suggest that the expansion of the universe is accelerating (e.g. Spergel et. al. 2003). It is thought that this acceleration is driven by a *dark-energy* component which, in its simplest incarnation, is described in terms of a fluid with pressure p related to the energy density, μ , by $p = w\mu$ with $w \approx -1$ at the present cosmic epoch. The continuity equation, $\dot{\mu} = -(1+w)\mu$ implies that for $w = -1$ the density is constant with time and, therefore, by Lorentz invariance, the fluid must be homogeneous. More generally, dark energy is modeled in terms of a scalar field which, under certain conditions, could be represented as a fluid with w varying with time. Such a fluid is not ruled out by observations. If this is the case, inhomogeneities in the dark energy component could develop. Since dark energy is inherently a relativistic entity, GR therefore should be invoked for a thorough treatment of small scale cosmological perturbations. Seen in this perspective self-similar solutions might be relevant for the description of structure formation in the universe. However, the solutions are quite limited in their applicability in a realistic model for the growth of structure in the presence of dark energy. Putting the subdominant baryonic matter aside, the problem of structure formation requires tracing the evolution of the gravitationally coupled system of collisionless dark matter and dark energy. Our solutions do not take this coupling into account. It is unclear whether self-similar evolution of cosmological perturbations in a two fluid system is possible at all. Further, we assume a strict equation of state of the form $p = w\mu$. This leads to an imaginary “sound” speed, $(\delta p/\delta\mu)^{1/2}$ for $w < 0$, while a more realistic model for dark energy in terms of scalar fields leads in general to a non-imaginary sound speed. Verertheless, because of the paucity of analytic solutions for time-dependent systems in GR, a treatment of systems with restricted symmetry is a worthwhile effort. Analytic study of these systems could also be useful in testing and calibrating numerical techniques for solving the GR equations.

6 ACKNOWLEDGMENT

The author especially thanks Amos Ori for many stimulating discussions on general relativity and self-similarity. He also thanks Ramy Brustein for useful discussions.

REFERENCES

- Bardeen J.M., 1965, *Stability and Dynamics of Spherically Symmetric Mass in General Relativity*, PhD thesis, California Institute of Technology
 Bardeen J.M., 1980, PhRvD, 22, 1882
 Bertschinger E., 1985, ApJS, 58, 39
 Cahil M.E., Taub A. H., 1971, Commun. math. phys. 21, 1
 Carr B.J., Hawking S.W., 1974, MNRAS, 168, 399
 Carr B.J., Yahil A., 1990, ApJ, 360, 330
 Carr B.J., Coley A.A., 2000, PhRvD, 62, 4023
 Chuzhoy L., Nusser A., 2000, MNRAS, 319, 797
 Fillmore J.A., Goldreich P., 1984, ApJ, 281,1
 Landau L.D., Lifshitz E.M., 1975, *The Classical Theory of Fields*, Elsevier

- Ori A. Piran T., 1990, PhRvD, 42, 1068
 Peebles P.J.E, 1993, *Principles of Physical Cosmology*, Princeton University Press
 Spergel D.N. et al., 2003, ApJS, 148, 175